



# Lawrence Berkeley Laboratory

UNIVERSITY OF CALIFORNIA

## Materials & Chemical Sciences Division

Submitted to Journal of Applied Catalysis

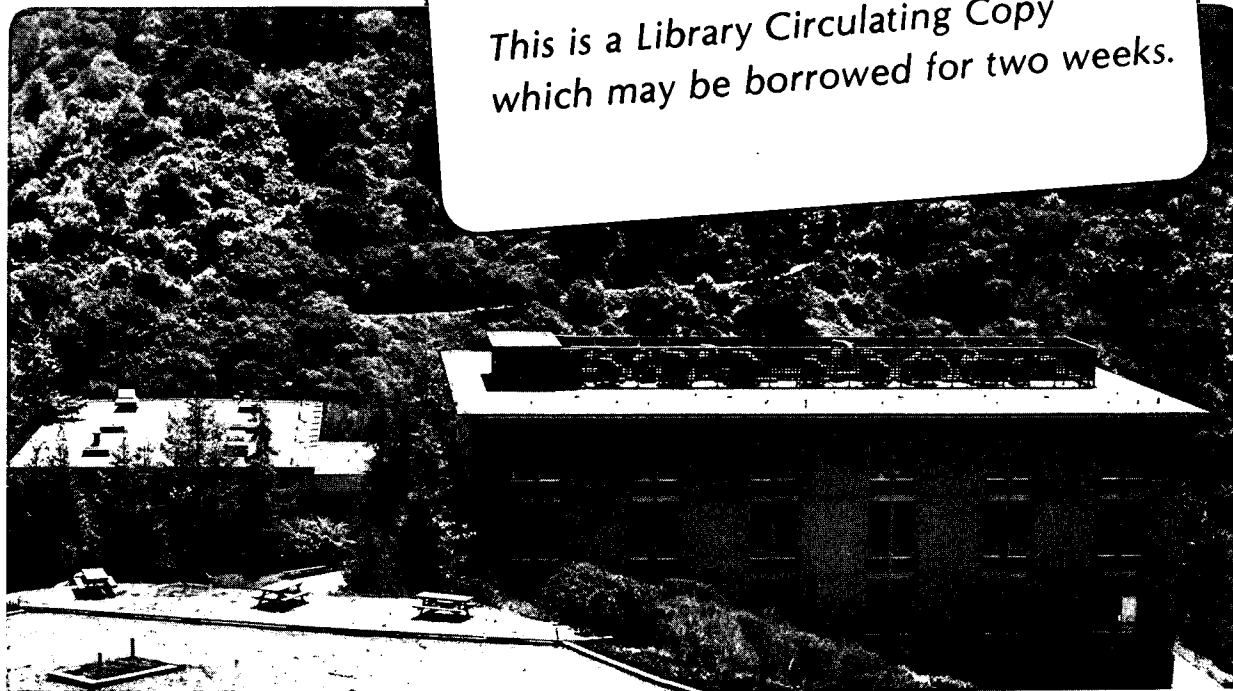
### Influence of Phosphorus in Vanadium-Containing Catalysts for NO<sub>x</sub> Removal

J. Blanco, P. Avila, C. Barthelemy, A. Bahamonde,  
J.A. Odriozola, J.F. Garcia de la Banda, and H. Heinemann

June 1989

TWO-WEEK LOAN COPY

*This is a Library Circulating Copy  
which may be borrowed for two weeks.*



LBL-27101  
c.2

## **DISCLAIMER**

This document was prepared as an account of work sponsored by the United States Government. While this document is believed to contain correct information, neither the United States Government nor any agency thereof, nor the Regents of the University of California, nor any of their employees, makes any warranty, express or implied, or assumes any legal responsibility for the accuracy, completeness, or usefulness of any information, apparatus, product, or process disclosed, or represents that its use would not infringe privately owned rights. Reference herein to any specific commercial product, process, or service by its trade name, trademark, manufacturer, or otherwise, does not necessarily constitute or imply its endorsement, recommendation, or favoring by the United States Government or any agency thereof, or the Regents of the University of California. The views and opinions of authors expressed herein do not necessarily state or reflect those of the United States Government or any agency thereof or the Regents of the University of California.

INFLUENCE OF PHOSPHORUS IN VANADIUM - CONTAINING  
CATALYSTS FOR NO<sub>x</sub> REMOVAL

J. Blanco, P. Avila, C. Barthelemy<sup>1</sup>,  
A. Bahamonde, J.A. Odriozola<sup>2</sup>,  
J.F. Garcia de la Banda, and H. Heinemann<sup>3</sup>

Instituto de Catalisis y Petroleoquimica, CSIC, Serrano 119, 28006-Madrid, Spain

<sup>1</sup> Universidad Nacional de Educacion a Distancia, Madrid, Spain

<sup>2</sup> Dept. de Quimica Inorganica, Univ. de Sevilla, Spain

<sup>3</sup> Lawrence Berkeley Laboratory, University of California, Berkeley, California, U.S.A.

## ABSTRACT

The influence of  $H_3PO_4$  on the catalytic activity of a vanadium-tungsten oxide-titania-based catalyst for the selective catalytic reduction (SCR) of nitrogen oxides with  $NH_3$  has been studied in a pseudoadiabatic fixed bed reactor. An activity decrease due to the presence of phosphorus has been observed as well as an increase in the crushing strength of the pellets. A chemical interaction between the active solid, the  $V_2O_5$ -based catalyst, and the extrusion binder,  $H_3PO_4$ , has been demonstrated by XPS and XRD. This interaction substantially decreases the concentration of vanadium species at the surface leading to the observed decrease in activity at temperatures between 250 and 300°C. However, at higher temperatures an activity increase takes place as a result of higher process selectivity to the SCR reaction.

## INTRODUCTION

The nitrogen oxides present in nitric acid plant tail gases are sources of air pollution. Although  $NO_x$  can be reduced to  $N_2$  with the use of reducing gases such as  $CH_4$ ,  $H_2$ , and  $CO$ , these gases are readily consumed by reaction with the oxygen present in tail gases.  $NH_3$  is a more economical reducing agent for a gas with a high  $O_2/NO_x$  ratio. This reaction has been extensively studied [1], mainly for use in the pollution abatement of tail gases from thermal power stations [2].

As has previously been pointed out [3], the differences between the tail gases from  $HNO_3$  plants and thermal power stations are mainly three:

- a) There are no  $SO_2$  and no suspended particles in  $HNO_3$  plant gases.

- b) The concentration of  $\text{NO}_x$  is higher ( $\text{NO}_x \approx 3000$  ppm).
- c) There is a higher proportion of  $\text{NO}_2$  (the ratio  $\text{NO}_2/\text{NO} \approx 1$ ).

These differences may considerably affect the catalyst behavior during the process, either by deactivation [4] or by enhancing the activity for the global process [5,6].

Various catalyst systems have been described in the literature for the SCR reaction. The most promising, from an industrial point of view, is  $\text{V}_2\text{O}_5$  [1] preferably supported on titania. A mechanism involving reduction of  $\text{V}_2\text{O}_5$  by  $\text{NH}_3$  and reoxidation by  $\text{NO}_x$  spilled over from titania has been proposed in a companion paper [32].

The characterization of the supported vanadium species by different techniques is relevant. Studies have been published on the use of EXAFS [7,8], HREM [9] and XPS [10,11] and kinetic studies have been directed to the elucidation of the reaction mechanism [12,13,14,15], in some cases supported by theoretical approaches [16]. Methods of preparation of titania-supported  $\text{V}_2\text{O}_5$  with improved redox properties [17] have been disclosed. However, an understanding of how extrusion binders modify the surface properties of the active solid is less apparent although, as Baiker et al. pointed out using  $\text{MoO}_3$  [18] and  $\text{V}_2\text{O}_5/\text{SiO}_2$  catalysts [19], the structural properties and catalyst morphology play an important role in this reaction under the working conditions used.

Commercial  $\text{V}_2\text{O}_5$ /titania catalysts consist of honeycombs, which are not subject to plugging by entrained solids and subsequent pressure drop. For nitric acid plants extruded pellets could be used which are substantially cheaper. However, vanadia-titania pellets are soft and subject to abrasion at high space velocities unless they can be hardened.

The use of inorganic acids as extrusion binders is common [20] for improving the mechanical strength of catalyst pellets. For titania-vanadia catalysts, only a brief reference in the patent literature was found [21] in which it was recommended to avoid the use of  $H_3PO_4$ , when the catalyst is used in the SCR process.

In this paper we compare the catalytic activity of catalysts that have been extruded with  $H_3PO_4$  for the  $NO_x + NH_3 + O_2$  reaction. Hg porosimetry, X-ray photoelectron spectroscopy (XPS) and X-ray diffraction (XRD) have been used as tools for the understanding of the surface modification as a function of the extrusion process.

## EXPERIMENTAL

### Catalysts

A titanium dioxide-vanadium oxide-tungsten oxide powder in which the atomic ratio of the metallic elements is 90:8:2 has been prepared. This powder has been extruded with  $H_3PO_4$  in such a way that a series of catalysts with the same Ti:V:W atomic ratio and variable phosphorus content has been obtained in order to investigate the effect of phosphorus on the catalytic activity of this powder.

The active solid was prepared by adding aqueous solutions of ammonium metavanadate (Merck) and ammonium paratungstate (Prolabo) to a hydrated titanium dioxide gel ("Titanium hydroxide paste" CLDD 1727, Tioxide) the characteristics of which are shown in Table 1. The resulting slurry was heated to dryness and ground to a particle size less than 0.250 mm. In order to prepare the extruded catalysts,  $H_3PO_4$  aqueous solutions at variable concentrations (0-14M) were added to the active powder; the relative amount of solid sample and phosphoric solution was chosen in such a way that the viscosity of the obtained slurry was always about 500,000 cps. After extrusion, the material was dried at room temperature for 10 hours and then at 110°C for 12 hours. Finally, the solid was treated in air at 500°C during 4 hours.

### Catalytic Activity

The catalytic activity measurements were carried out in a pseudoadiabatic fixed bed reactor operating in an integral regime. A schematic representation of the reactor is shown in Fig. 1. Since formation of ammonium salts between  $\text{NO}_x$  and  $\text{NH}_3$  is favored at temperatures lower than 425 K [22], the ammonia was fed separately directly into the reactor.

The  $\text{NO}_2$ :NO molar ratio at the reactor inlet was ca. 1; this ratio was kept constant by mixing NO and  $\text{O}_2$  upstream of the catalytic bed.

A chemiluminescence apparatus LUMINOX (B.O.C.) was used to measure NO and  $\text{NO}_2$  concentrations in the inlet and outlet reactor flow. The ammonia and  $\text{N}_2\text{O}$  concentrations were measured by an IR spectrophotometer MIRAN 1A (Foxboro). Since the  $\text{N}_2\text{O}$  concentration in the reactor outlet was always less than 5%, this compound was not taken into consideration for further analyses.

The operating conditions (Table 2) were selected to simulate the characteristics of tail gases of nitric acid plants.

### Apparatus

X-ray fluorescence analyses were carried out on the catalysts to determine the absolute amounts of Ti, V, W, P, and S. A sequence spectrometer SRS 300 was used.

The X-ray diffraction pattern (XRD) of the catalysts was obtained in a Phillips APD 10 with a graphite monochromator and Cu  $K\alpha$  radiation.

The XPS spectra were obtained in an ultra high vacuum apparatus previously described [23]. (In brief it consists of an ultra high vacuum

chamber with a built-in high pressure cell which allows switching the sample from the high pressure cell to the UHV system without exposing it to the air. The XPS spectra were recorded using a cylindrical mirror analyzer and Mg K $\alpha$  radiation [40 mA, 10 kV]. For the spectra calibration the Au [4f 7/2] line at 83.8 eV and the Ti [2p 3/2] one at 458.5 eV were used.)

The crushing strength was determined in a dynamometer Chatillon model DPP.

## RESULTS AND DISCUSSION

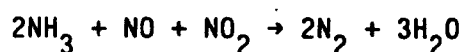
The influence of phosphoric acid content on the performance of a vanadium oxide-based catalyst for the removal of NO<sub>2</sub> from tail gases of nitric acid plants has been studied in a series of tests in which the only variable considered is the amount of phosphorus present in the pellets. The composition and physical properties of the catalysts studied are shown in Table 3.

It is obvious from these data that the mechanical strength of the pellets increases with the phosphorus content; the crushing strength and the apparent density of the solid increases while the specific surface area and the total pore volume decreases. Plots of the cumulative mercury intrusion volume against the mean pore radius are shown in Fig. 2. It is observed that the average pore radius is around 1,500 Å for the whole series. Since the particle size of the starting TiO<sub>2</sub> gel is 7  $\pm$  1  $\mu$ m, it may be assumed that these pores are the interparticle spaces and not actual pores.

Results presented in Fig. 2 indicate that the phosphorus is mainly inside these interparticle spaces. Its binding effect is due to the filling of these spaces, following a compacting mechanism similar to that described by Capes as "mobile liquid bonding" [20].



Using this series of catalysts, the influence of the reaction temperature has been investigated. The molar conversion of each reactant (NO, NO<sub>2</sub>, and NH<sub>3</sub>) as well as the total NO<sub>x</sub> conversion as a function of the reaction temperature is plotted in Fig. 3 for the phosphorus-free catalyst (PO). For this catalyst, as the temperature increases from 250 to 300°C, the molar conversion of NO, NO<sub>2</sub>, and NH<sub>3</sub> increases according to the following global stoichiometry:



At temperatures above 330°C the molar conversion of NO drops with increasing temperature of reaction while NO<sub>2</sub> and NH<sub>3</sub> conversions still increase. This behavior leads to a maximum in the NO<sub>x</sub> conversion curve between 300 and 350°C. The change of the global NO<sub>x</sub> conversion versus reaction temperature for each catalyst in this series is shown in Fig. 4, under the previously mentioned operating conditions. It is shown that when the catalyst pellets are prepared by extrusion of the active phase with H<sub>3</sub>PO<sub>4</sub>, the decline in NO molar conversion at the highest reaction temperature is less than in the case of the phosphorus free catalyst. However, the total NO<sub>x</sub> conversion at low temperatures depends on the phosphorus content and is significantly lower in the case of the high phosphorus content catalysts. The higher the phosphorus content, the lower the catalytic activity probably because more of the reducible V<sub>2</sub>O<sub>5</sub> species are converted to non-reducible phosphates.

From these results, when the catalyst was prepared with a phosphoric acid concentration lower than 7 M, catalysts with acceptable hardness could be obtained, giving NO<sub>x</sub> conversion levels at 350°C close to those obtained with catalysts containing no phosphoric acid.

Moreover, when the reaction temperature is higher than 350°C, the catalysts with low H<sub>3</sub>PO<sub>4</sub> content gave NO<sub>x</sub> conversion levels higher than those without phosphoric acid. This indicates that the presence of such acid results in a decrease of the NH<sub>3</sub> oxidation

reaction by the oxygen present in the reaction mixture. Therefore, the selectivity for the reduction of  $\text{NO}_x$  by  $\text{NH}_3$  is increased.

In summary, it may be said that the extrusion with phosphoric acid has two effects: it increases the mechanical resistance of the pellets and decreases the catalytic activity of both the  $\text{NO}_x$  reduction reaction and the  $\text{NH}_3$  oxidation by the  $\text{O}_2$  present in the reaction mixture. The last reaction is responsible for the decrease in  $\text{NO}_x$  conversion when reaction temperature increases.

In a first attempt to elucidate the modifications introduced at the catalyst surface with the extrusion process, XPS spectra of the catalysts have been obtained. The  $\text{O}(1s)$ ,  $\text{V}(2p)$ ,  $\text{W}(4f)$ ,  $\text{Ti}(2p)$ ,  $\text{S}(2p)$ ,  $\text{C}(1s)$ , and  $\text{Au}(4f)$  signals have been recorded. The sulfur species present in the catalysts, Table 3, were impossible to detect even at high collection times (45 minutes); the  $\text{C}(1s)$  and the  $\text{Au}(4f)$  signals were recorded for calibration purposes, although the  $\text{C}(1s)$  was not used due to the impossibility of discriminating between the signal coming from the support, a gold foil, and the one coming from the sample.

Figure 5 shows the  $\text{V}(2p)$  region for the P0 and P2 catalysts. The  $\text{V}(2p\ 3/2)$  for the air stabilized P0 sample peaks at 517.0 eV in good agreement with the reported values for vanadia/titania catalysts [10,11,24,25]. Lars and Anderson, who standardized their spectra to the  $\text{O}(1s)$  peak at 529.6 eV, state that peaks at 516.6 eV are obtained for  $\text{V}_2\text{O}_5$  [17]. Considering that our standardizing method allows us a ca. 0.4 eV shift towards higher binding energies [in our case the  $\text{O}(1s)$  signal when referred to the  $\text{Ti}(2p\ 3/2)$  one peaks at 530.0 eV], we could assign the peak at 517.0 eV to the presence of  $\text{V}_2\text{O}_5$ . This assignment agrees fairly well with the XPS spectra of crystalline  $\text{V}_2\text{O}_5$  and of the vanadia-titania system described by J.L.G. Fierro et al. [26].

On the other hand, the  $\text{V}(2p\ 3/2)$  feature for the P2 catalyst, Fig. 5, is less resolved than in the case of the P0 one. Considering the

differences in binding energies for  $V^{5+}$ ,  $V^{4+}$ , and  $V^{3+}$ , ca. 0.5 eV [25], it is hard to unequivocally assign this peak to a single vanadium species, particularly if one considers that the full width at half maximum (FWHM) is bigger than in the case of the P0 catalyst. However, the presence of  $V^{5+}$  species cannot be disregarded.

Due to the severe overlapping of the V(2p 1/2) with the O(1s) X-ray satellites, coming from the non-monochromatized X-ray source used, any discussion concerning this feature is worthless for most of the recorded spectra. However, such an overlapping provides some valuable quantitative information; if one compares the relative intensity of both the O(1s) satellites peak and the V(2p 3/2) peak, it is possible to conclude that even with the same bulk Ti/V atomic ratio, the amount of vanadium species present at the surface has to be considerably less in the case of sample P2 than in the case of P0.

The O(1s) signal for the P0 catalyst peaks at 530.0 eV, while when phosphorus is present (P2 catalyst) it peaks at 530.7 eV (Fig. 6). In addition the O(1s) signal for the P0 catalyst shows a tail extending over the high binding energy side of the spectrum that is not present in the P2 catalyst. This tail is eliminated by heating at reaction temperatures, e.g., 300°C which could mean that hydroxyl species are responsible for this feature. The peak at 350.0 eV should be ascribed to oxide ions, and the peak at 530.7 eV has to be associated with oxygen atoms linked to the phosphorus atoms present in the P2 sample. As the P(2p) peaks at 132.7 eV, it should be ascribed to phosphate species [27].

On the basis of these results we conclude that the surface concentration of vanadium decreases when the catalyst is extruded with phosphoric acid and the surface of the  $H_3PO_4$ -extruded catalysts is mainly composed of phosphate species, while the metallic oxides, if present, are under a phosphate layer.

In order to elucidate the effect produced by the  $H_3PO_4$  on the

TiO<sub>2</sub> and to know whether the vanadium species are present either as oxides or as phosphate salts, XRD measurements have been carried out.

Figure 7 gives the diffraction pattern belonging to the TiO<sub>2</sub> paste used as carrier of the catalysts. Signals in this pattern coincide with those of the ASTM card 21-1272 belonging to TiO<sub>2</sub> (anatase). The average size of the crystals of TiO<sub>2</sub> (anatase) in each sample has been determined by the method described in [26]. The values are given in Table 4.

These results indicate that when the paste is treated at 500°C an appreciable increase in the size of the crystals takes place. This increase does not appear when the catalyst is extruded with phosphoric acid, which indicates that the H<sub>3</sub>PO<sub>4</sub> inhibits the crystallization of the anatase when this material is submitted to a thermal treatment. Criado and Real observed a similar effect for the transformation of anatase to rutile due to the ions PO<sub>4</sub>H<sup>2-</sup> [28]. According to these authors, the ions are anchored on the surface of the TiO<sub>2</sub> through surface OH groups in the form of bidentate ligands.

In our case, the H<sub>3</sub>PO<sub>4</sub> could form similar polidentate ligands on the TiO<sub>2</sub> surface inhibiting the ionic mobility which is needed for the growing of the anatase crystals. The inhibition of crystallite growth offers an explanation for the relatively high activity at high temperature for low phosphorus content catalysts (Fig. 4).

XRD diffraction patterns for the catalyst series studied are shown in Fig. 8.

In general the presence of phosphorus in the catalyst inhibits the growing of anatase crystals and destroys the crystals of V<sub>2</sub>O<sub>5</sub> leading to the formation of new species. If the finished catalyst does not contain phosphorus (PO), maxima at d=4.38, 3.40, and 2.82 Å are observed in addition to the anatase peaks (O) in Fig. 8; these peaks

match the spectrum corresponding to  $V_2O_5$  (●), and again corroborate the presence of vanadium pentoxide crystallites in the P0 catalyst.

The formation of new chemical compounds by reaction of the aqueous phosphoric acid solution with the active solid is supported by the presence of new peaks in the XRD pattern of the  $H_3PO_4$ -treated samples. At low phosphorus content, P1, peaks at  $d=3.05$  and  $7.16$  Å are observed, these peaks being ascribed to  $\beta$ - $Ti(HPO_4)$ , (■) in Fig. 8. If the phosphorus content increases, new phases appear characterized by peaks at  $d=3.1$ ,  $1.9$ , and  $1.5$  Å, and  $d=3.40$ ,  $3.07$ , and  $5.18$  Å that should be ascribed to  $\alpha$  and  $\beta$ -vanadyl phosphate, respectively. These phases increase their concentration as the phosphorus content increases. At the highest phosphorus content (P3 catalyst), a new peak at  $2\theta$  ca.  $20^\circ$  appears, the assignation of which is not clear. According to literature data it could be ascribed either to a  $\beta^*$  phase (Hodnett et al [29]) or to a vanadyl pyrophosphate (Bordes et al. [30]).

Vanadyl phosphate in the absence of titania exhibits denox activity, which, however, rapidly declines. XRD spectra of spent  $V_2O_5$ - $TiO_2$  catalysts do not show the phosphate species which therefore may be unstable at the reaction conditions.

#### CONCLUSIONS:

From the above data it is concluded that the  $H_3PO_4$  treatment modifies the surface of the vanadia-containing catalyst. The formation of new solid phases that contains phosphate ions not only reduces the amount of vanadium species present at the surface (as demonstrated by XPS) but also modifies the catalyst composition at the surface changing its reducibility, as has been shown by ESR and TPR [31]. In another publication [32] it has been shown that the  $NO_x + NH_3$  reaction on  $V_2O_5$ -titania involves a redox mechanism. The behavior of the catalyst for the SCR of nitrogen oxides as a function of the temperature

is changed by the incorporation of phosphates. The increase in the crushing strength of the pellets is obtained as a result of the formation of phosphate phases probably present as polyphosphates.

The phosphorus compounds formed are mainly located in the interparticle spaces of the  $\text{TiO}_2$  grains, decreasing the porosity and inhibiting the growth of anatase crystals.

The effect of  $\text{H}_3\text{PO}_4$  on the two parameters we are interested in optimizing (crushing strength and catalytic activity) forces a compromise in the selection of the concentration of the acid needed for compacting the solids while maintaining good activity.

#### ACKNOWLEDGEMENTS

This work was supported by the CAICYT (Project No. 618/397) and the U.S.-Spain Joint Committee for Science and Technology. The authors also thank Repsol Petroleo S.A., and especially the deceased Dr. J. Marti, for the XRD spectra.

REFERENCES

1. H. Bosch and F. Janssen, CATALYSIS TODAY, 2, 369 (1988).
2. H.E. Cichanowicz, POWER ENG., Aug, 34 (1988).
3. P. Avila, J. Blanco, M. Moreno, Acts 9 Symp. Iberoam. Catal. Vol. II, 817, Lisboa (1984).
4. J. Blanco, P. Avila, AN. QUIM., 80 (2), 645 (1984).
5. P. Avila, A. Bahamonde, C. Barthelemy, J. Blanco, Acts 11 Symp. Iberoam. Catal. 1317, Mexico (1988).
6. G. Tuentner, W.F. van Leeuwen, L.J.M. Snepvangers, IND. ENG. CHEM. PROD. RES. DEV., 25, (4), 633 (1986).
7. R. Kozłowski, R.F. Pettifer, and J.M. Thomas, J. PHYS. CHEM., 87, 5176 (1983).
8. J. Haber, A. Kozłowska, and R. Kozłowski, J. CATAL., 102, 52 (1986).
9. Z.C. Kang and Q.X. Bao, APPL. CATAL. 26, 251 (1986).
10. G.C. Bond, J. Perez Zurita, and S. Flamerz, APPL. CATAL., 12, 353 (1986).
11. F.J. Gil-Llambias, A.M. Escudey, J.L.G. Fierro, and A. Lopez-Agudo, J. CATAL., 95, 520 (1985).
12. A. Miyamoto, K. Kobayashi, M. Inomata, and Y. Murakami, J. PHYS. CHEM., 86, 2945 (1982).

13. H. Bosch, F.J.J.G. Janssen, F.M.G. van der Kerkhof, J. Oldenziel, J.G. van Ommen, and J.R.H. Ross, APPL. CATAL., 25, 239 (1986).
14. J. Blanco, J.F. Garcia de la Banda, P. Avila, and F.V. Melo, J. PHYS. CHEM., 90, 4789 (1986).
15. F.J. Janssen, F.M. van der Kerkhof, H. Bosch, J.R. Ross, J. PHYS. CHEM. 91, 6633 (1987).
16. A. Miyamoto, M. Inomata, A. Hattori, T. Ui, and Y. Murakami, J. MOL. CATAL., 16, 315 (1982).
17. G.C. Bond, J. Perez Zurita, S. Flamerz, P.J. Gellings, H. Bosch, J.G. van Ommen, and B.J. Kip, APPL. CATAL., 22, 361 (1986).
18. A. Baiker, P. Dollenmeier, A. Reller, J. CATAL., 103, 394 (1987).
19. A. Baiker, P. Dollenmeier, M. Glinski, A. Reller, V.K. Sharma, J. CATAL., 111, 273 (1988).
20. C.E. Capes, HANDBOOK OF POWDER TECHNOLOGY.1. "Particle Size Enlargement." Elsevier ed. (1980).
21. U.S. Pat. 4.518.710.
22. W. Toering,, AIR POLLUTION BY NITROGEN OXIDES, T. Schneider and L. Grant eds., Elsevier Scientific Publ. Co. Amsterdam (1982).
23. G.A. Somorjai, CHEM. SOC. REV., 13, 321 (1984).
24. J. Haber, T. Machej, and T. Czeppe, SURFACE SCI., 151, 301 (1985).
25. S. Lars and T. Anderson, J. CHEM. SOC. FARADAY TRANS. I, 75, 1356 (1979).



26. J.L.G. Fierro, L.A. Arrua, J.M. Lopez Nieto, G. Kremenec, APPL. CATAL., 37, 323 (1988).
27. D. Briggs and M.P. Seah eds., PRACTICAL SURFACE ANALYSIS, John Wiley & Sons Ltd., New York (1983).
28. J. Criado, C. Real, J. CHEM. SOC. FAR. TRANS., 79, (1), 2765 (1983).
29. B.K. Hodnett, Ph. Bermanne, B. Delmon, APPL. CATAL., 6, 231 (1983).
30. E. Bordes, P. Courtine, J. CHEM. SOC. CHEM. COMM., 294 (1985).
31. J. Soria et al, J. CAT. (accepted for publication).
32. J.A. Odriozola, H. Heinemann, G.A. Somorjai, J.F. Garcia de la Banda, and P. Pereira, J. CAT. (accepted for publication).

TABLE 1

Characteristics of the "Titanium Hydroxide Paste"  
CLDD 1727 (Tioxide)

---

Composition (% by weight):

$\text{TiO}_2$  . . . . 36.0

$\text{H}_2\text{O}$  . . . . 56.0

$\text{SO}_4^{=}$  . . . . 8.0

pH . . . . 1.5

Particle size . . . .  $7 \pm 1 \mu\text{m}$

---

TABLE 2  
Catalytic Activity Operating Conditions

---

Total flow of gases:	$3.0 \text{ NL.min}^{-1}$
G.H.S.V.:	$40,000 \text{ h}^{-1}$
Feed Composition:	
	$\text{NO}_x$ 3000 ppm
	$\text{NH}_3$ 3000 ppm
	$\text{O}_2$ 3% by volume
	$\text{N}_2$ to balance
$\text{NO}_2/\text{NO}$ molar ratio:	$1.0 \pm 0.1$
Reaction temperature:	525-725K

---

TABLE 3  
Composition and Physical Properties of the Prepared Catalysts

Catalyst	Composition (% by weight)					Atomic Ratio P/(Ti+V+W)	Bulk Density g/cm <sup>3</sup>	S <sub>BET</sub> m <sup>2</sup> /g	V <sub>pore</sub> cm <sup>3</sup> /g	Crushing Strength K <sub>p</sub>
	Ti	V	W	P	S					
P 0	49.4	4.6	4.4	--	1.2	--	1.0	63.8	0.69	0
P 1	35.0	3.4	3.2	12.3	1.1	0.49	1.3	12.7	0.46	4.3
P 2	32.0	3.2	3.0	14.7	1.0	0.63	1.5	7.7	0.30	8.3
P 3	28.6	2.9	2.7	17.9	0.9	0.86	1.8	3.1	0.18	16.8
P 4	24.2	2.7	2.5	21.6	0.8	1.21	2.0	1.0	0.10	30.2

TABLE 4  
Crystal size of  $\text{TiO}_2$  (anatase)

Sample	$L_c$ (Å)
a. - Dried paste	66.9
b. - Paste treated at $500^\circ\text{C}$	134.5
c. - Paste with $\text{H}_3\text{PO}_4$ , treated at $500^\circ\text{C}$	67

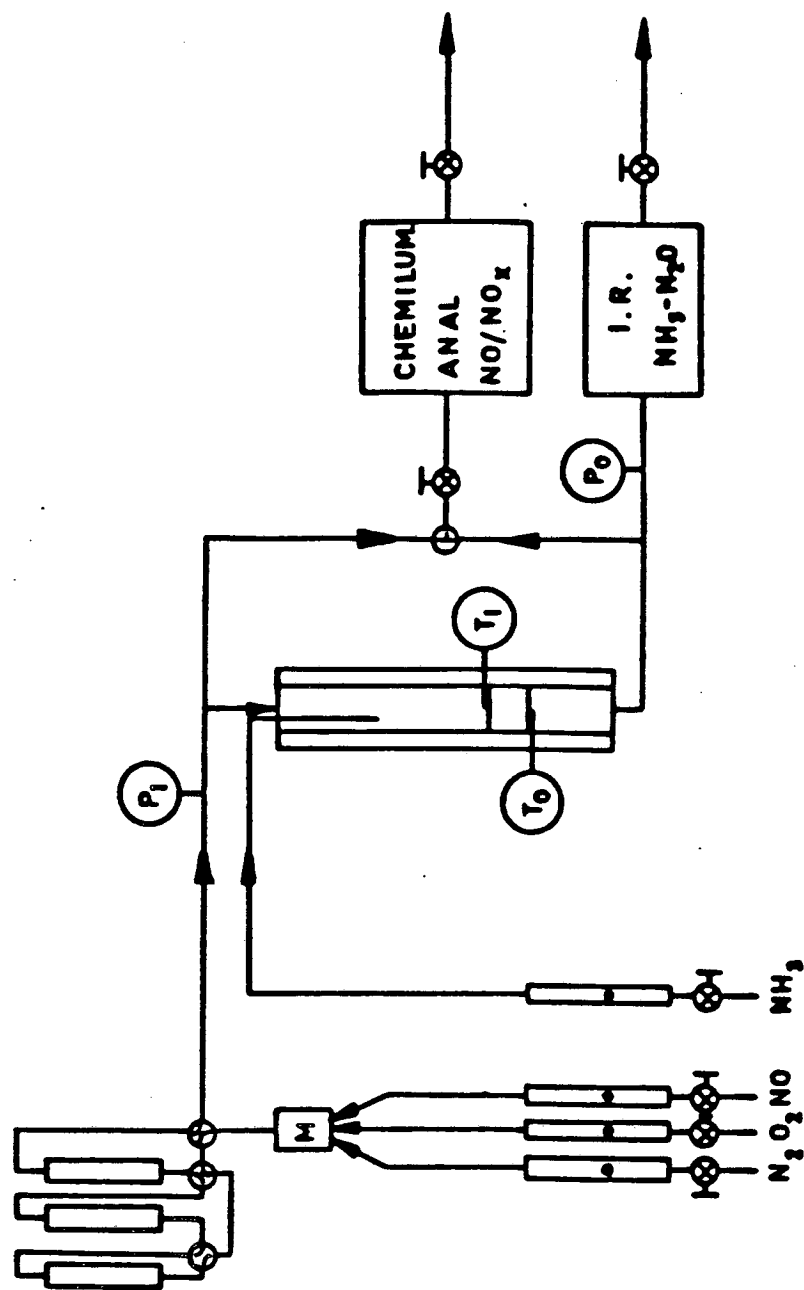


Fig. 1. Schematic flow diagram of the experimental system.

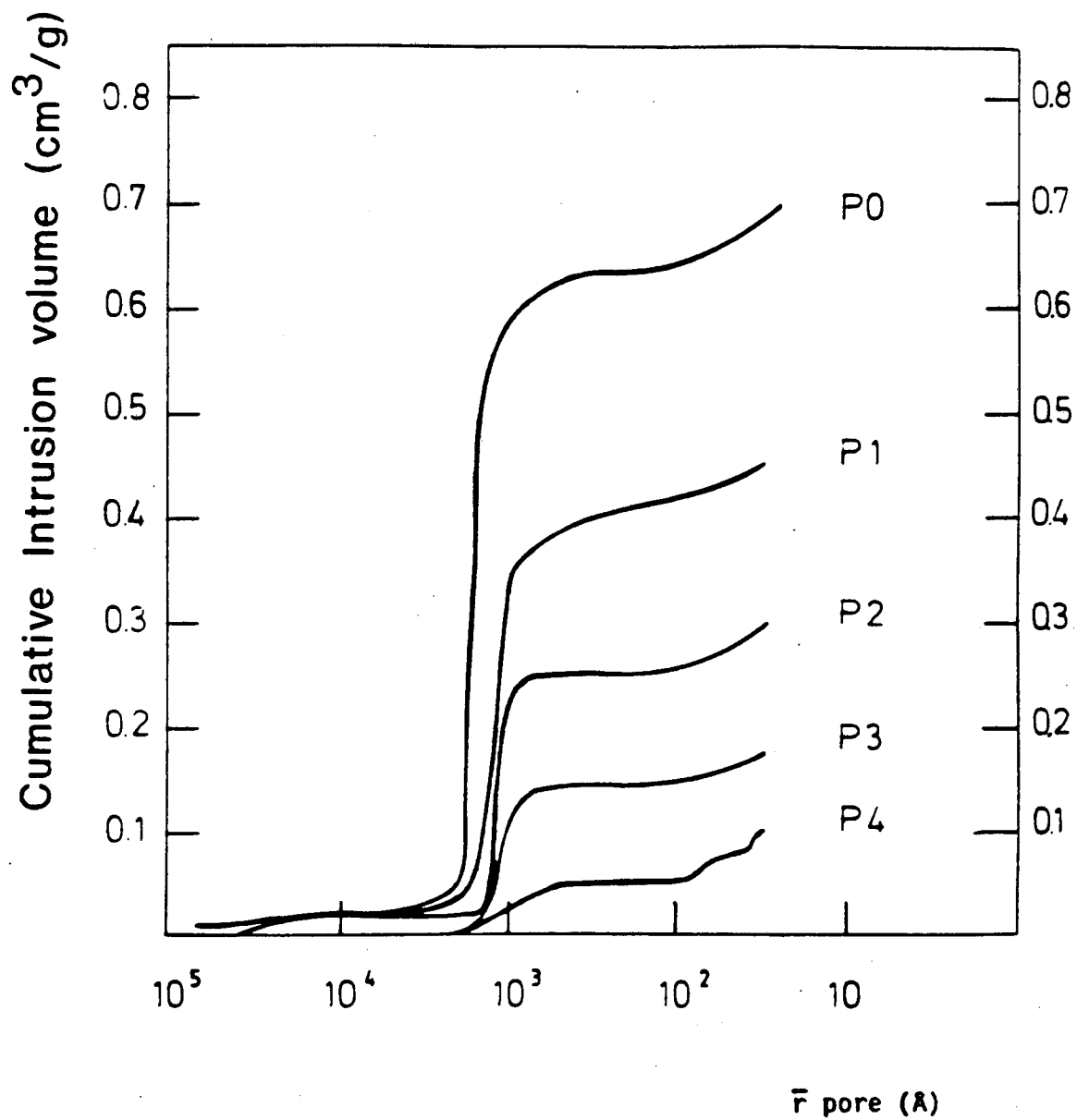


Fig. 2. Influence of phosphorus content on the porosity of series "p" catalysts.

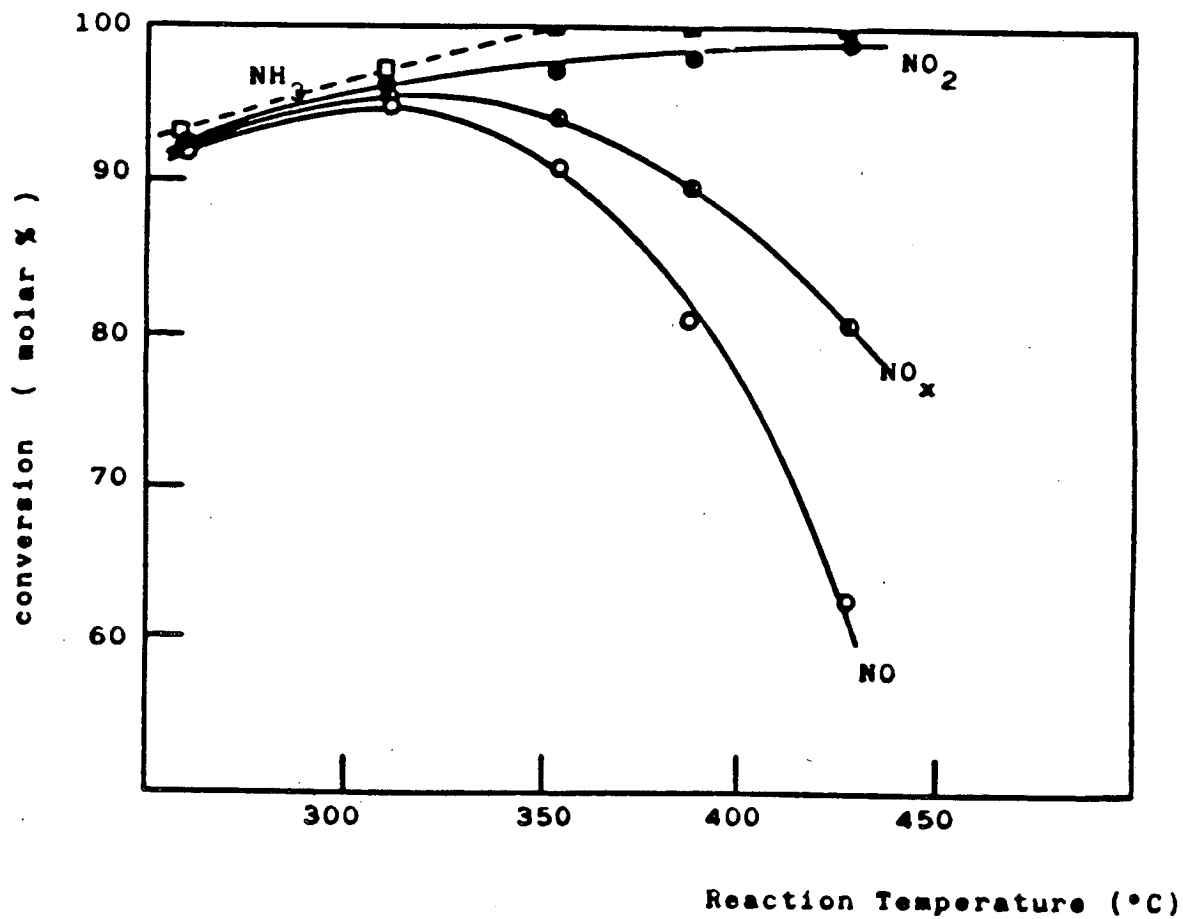


Fig. 3. Influence of the reaction temperature on the conversion of NH<sub>3</sub> (□), NO (○), NO<sub>2</sub> (●), and NO<sub>x</sub> (●). Catalyst: PO. GHSV: 40.000h<sup>-1</sup>. Feed composition: NO<sub>x</sub>:3000ppm (NO=NO<sub>2</sub>=1500ppm), NH<sub>3</sub> (3000ppm), O<sub>2</sub>:3% vol, N<sub>2</sub>:balance.



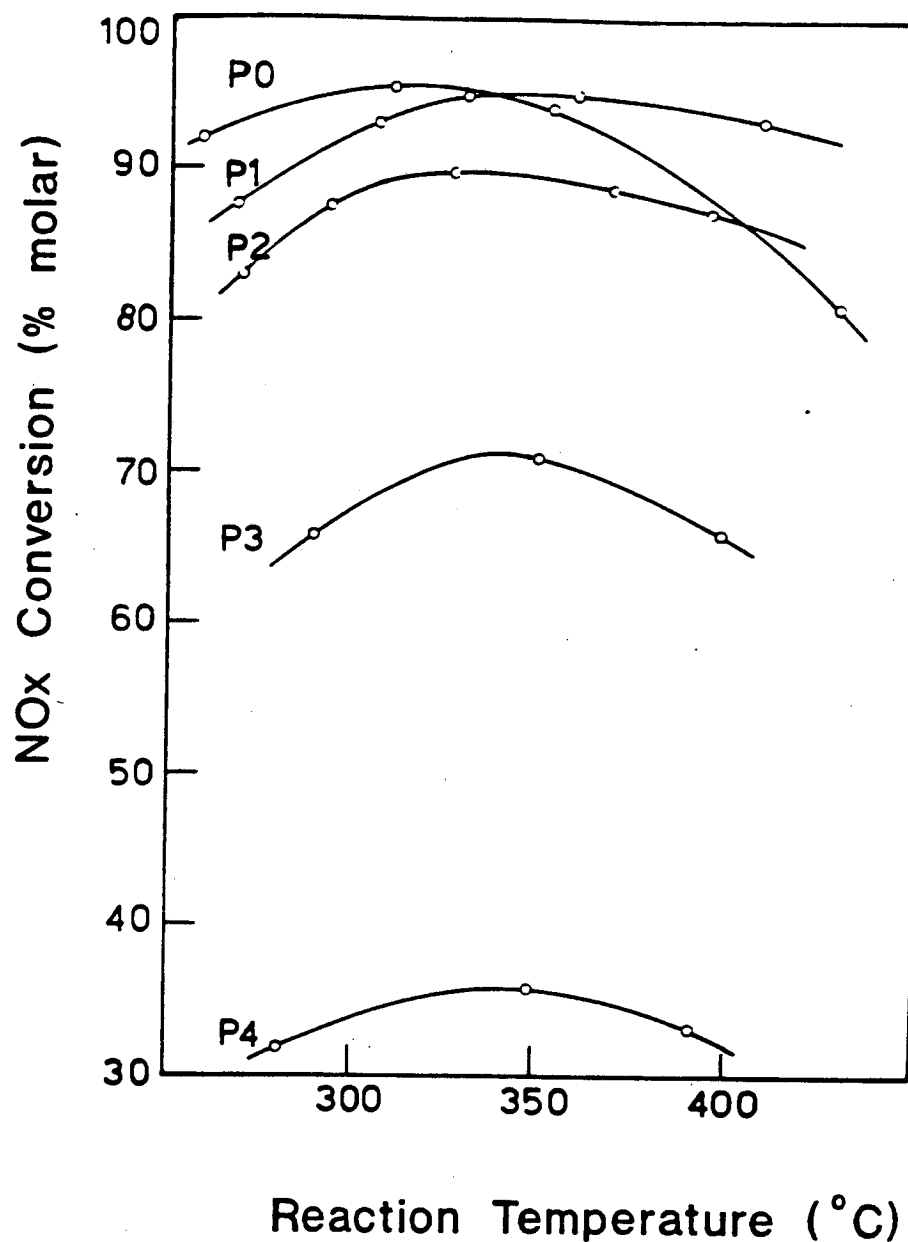


Fig. 4. Influence of the reaction temperature on the  $\text{NO}_x$  conversion for the catalysts of the series P. Operating conditions:  $\text{GHSV}=40000 \text{ h}^{-1}$ ; Feed composition:  $\text{NO}_x=3000\text{ppm}$ , ( $\text{NO}=\text{NO}_2=1500\text{ppm}$ );  $\text{NH}_3=3000\text{ppm}$ ;  $\text{O}_2=3\% \text{ vol}$ ;  $\text{N}_2=\text{balance}$ .

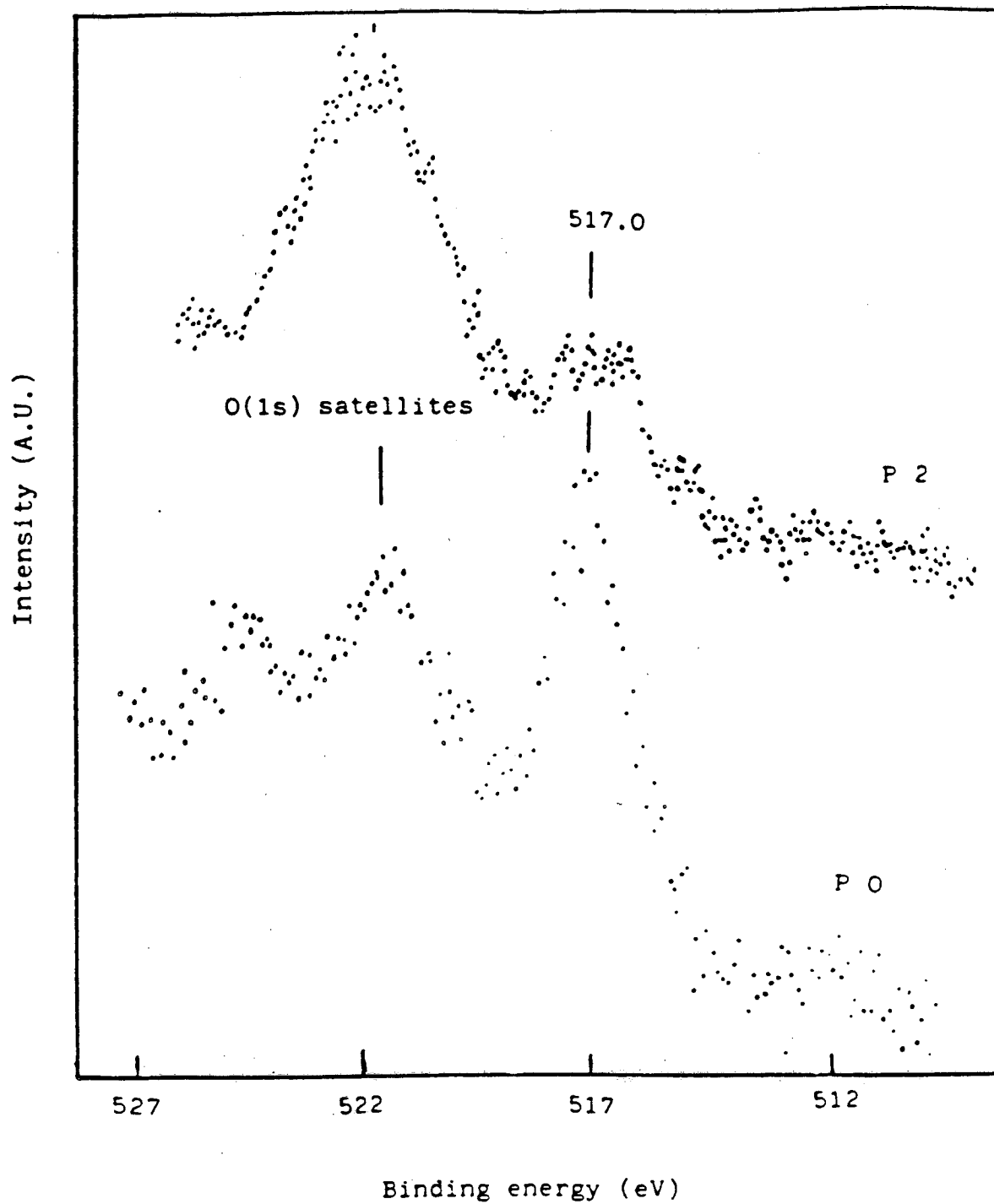


Fig. 5. V(2p) spectra for the air stabilized P 0 and P 2 catalysts.

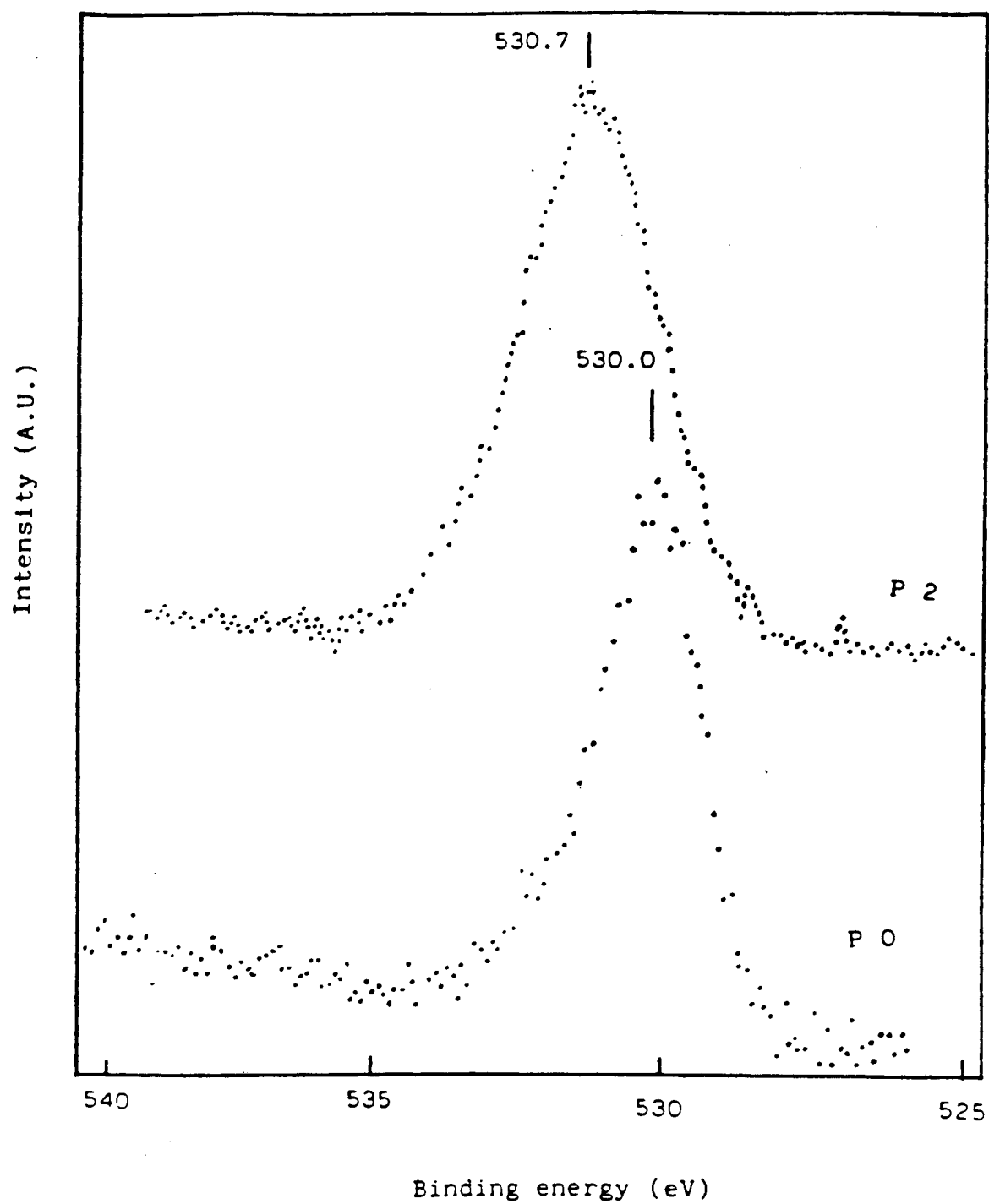


Fig. 6.0(1s) spectra for the air stabilized P 0 and P 2 catalysts.

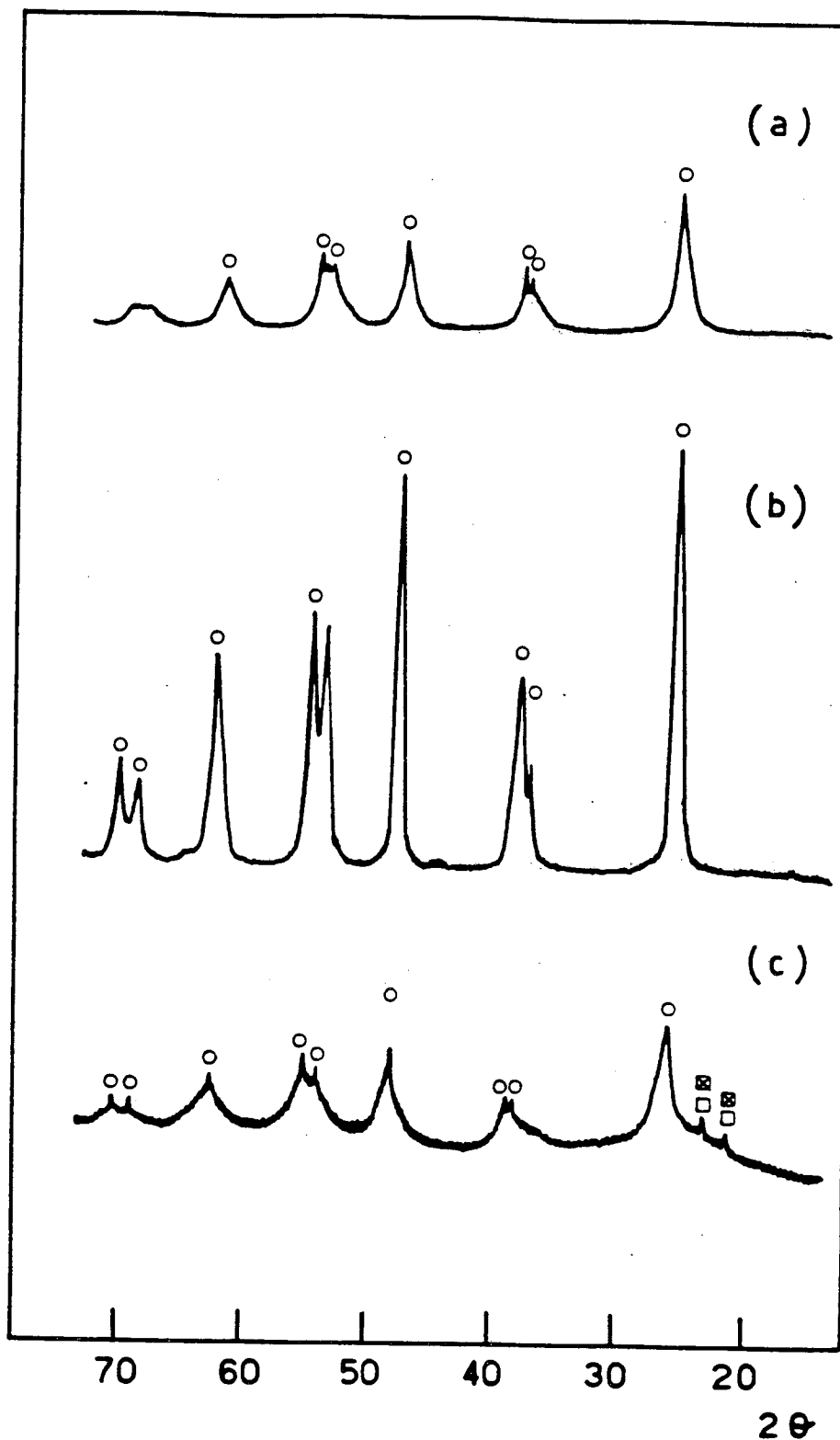


Fig. 7. X-ray diffraction diagrams of: a)  $\text{TiO}_2$  hydrated gel; treated at 373 K in air; b)  $\text{TiO}_2$  hydrated gel, treated at 773 K in air, and c)  $\text{TiO}_2$  hydrated gel extruded with  $\text{H}_3\text{PO}_4$  solution, treated at 773 K in air.

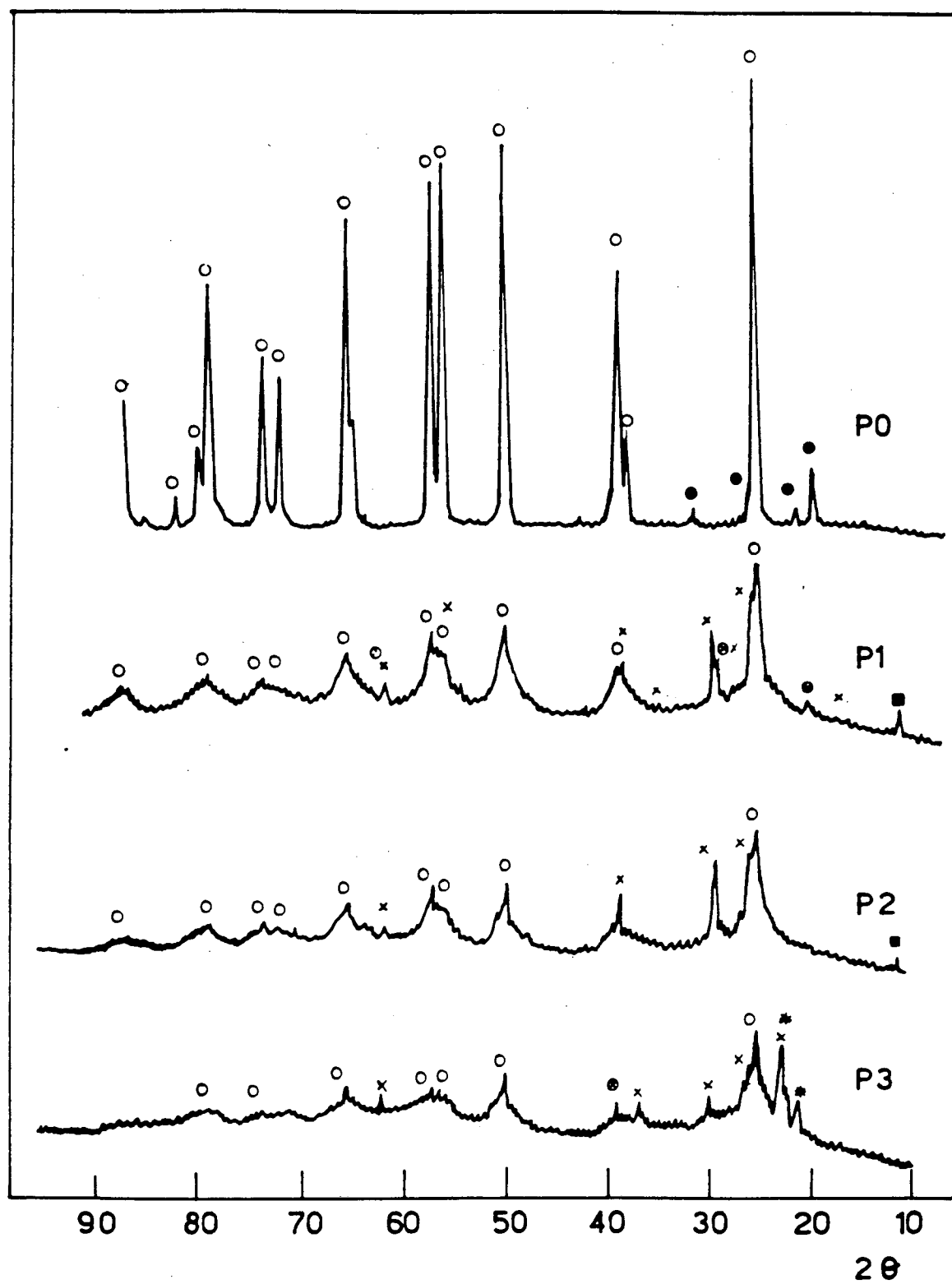


Fig. 8. X-ray diffraction diagrams of series P catalyst, treated at 773 K in air.

LAWRENCE BERKELEY LABORATORY  
TECHNICAL INFORMATION DEPARTMENT  
1 CYCLOTRON ROAD  
BERKELEY, CALIFORNIA 94720